Context-dependent environmental adaptation of olfactory receptor abundances

Tiberiu Teşileanu[a,b,1], Simona Cocco[c], Rémi Monasson[d], and Vijay Balasubramanian[a,b]

[a]Initiative for the Theoretical Sciences, The Graduate Center, CUNY, New York, NY 10016
[b]David Rittenhouse Laboratories, University of Pennsylvania, Philadelphia, PA 19104
[c]Laboratoire de Physique Statistique, École Normale Supérieure and CNRS UMR 8550, PSL Research, UPMC Sorbonne Université, Paris, France
[d]Laboratoire de Physique Théorique, École Normale Supérieure and CNRS UMR 8550, PSL Research, UPMC Sorbonne Université, Paris, France

May 8, 2018

Abstract

Olfactory receptor usage is highly non-uniform, with some receptor types being orders of magnitude more abundant than others. In mammals, the receptor neurons are replaced regularly, and the receptor distribution changes in response to olfactory experience. The observed changes are mysteriously context-dependent, with increased exposure to odorants leading variously to increased, decreased or unchanged abundance of activated receptors. We propose a theoretical model that explains these observations: the receptor distribution is tuned to efficiently encode information about the olfactory environment. This adaptation occurs before olfactory signals are decorrelated, leading to a new regime of efficient coding in which the optimal receptor distribution is sensitive to the global context of the correlated responses of all receptor types in the population. We demonstrate how this effect reproduces the context-dependence seen in experiments. We also show that the optimal receptor distribution can be achieved by following simple dynamical rules for neural birth and death processes.

1 Introduction

Olfaction is hard: according to some estimates, there may be tens of billions of odorants—volatile molecules that exhibit an odor—that can be encountered in nature [1]. The olfactory system has the daunting task of detecting these molecules in minute concentrations in order to guide an animal towards food or away from danger. To do so, the olfactory epithelium in mammals and the antennae in insects are populated with large numbers of olfactory sensory neurons (OSNs), each of which expresses a single kind of olfactory receptor. Each type of olfactory receptor binds to many different odorants, and each odorant activates many different receptors, leading to a complex encoding of olfactory scenes [2]. Olfactory receptors form the largest known gene family in mammalian genomes, with hundreds to thousands of members, owing perhaps to the importance that olfaction has for an animal's fitness [3, 4, 5]. Independently-evolved large olfactory receptor families can also be found in insects [6].

In mammals, the olfactory epithelium experiences neural degeneration and neurogenesis, resulting in replacement of the OSNs every few weeks [7]. This means that the relative abundances of different receptor types may be modulated by the olfactory environment. Indeed, the distribution of receptors in mammals has been found to depend on olfactory experience [8, 9, 10, 11, 12, 13]. The relation between environmental changes and changes in receptor abundances depends on the context of the experiments in a way that is not yet understood, with increased exposure to ligands sometimes leading to increased abundance of receptors, sometimes to decreased abundance, and sometimes having no effect [9, 10, 12, 13]. Moreover, the reasons behind this adaptation are unknown [13].

In this paper, we propose a solution to these puzzles by hypothesizing that the distribution of receptors in the olfactory epithelium is chosen to maximize the amount of information that the animal gets about its olfactory environment. This is a variant of the efficient-coding hypothesis [14, 15] that has already been used successfully for other sensory modalities, such as vision and audition [16, 17, 18, 19, 20, 21, 22]. It has also been suggested that olfactory sensing might be adapted to the sparsity of odor mixtures [23, 24, 25] and that receptor-odorant affinities might be specially adapted to odors in the environment [26, 27, 28].

In contrast to earlier work, here we take the receptor-odorant affinities as given and instead propose a model for the quantitative distribution of olfactory sensory neurons by receptor type. Qualitatively, our hypothesis that the neural responses present a maximally-informative picture of the olfactory environment leads to the prediction that, in a noisy odor environment, the distribution of receptor types that is best adapted to natural olfactory scenes will be highly non-uniform, but reproducible given fixed receptor affinities and environmental odor statistics. The adaptation could happen during the lifetime of an individual, in response to the statistics of odors encountered by the organism, if such changes are allowed by the biology (*e.g.,* in mammals); or it could happen over evolutionary times, in response to the typical odor environments encountered by organisms of the same species. As noted above, short time-scale adaptation has already been observed in experiments [8, 9, 10, 11, 12, 13]. Furthermore, Ibarra-Soria *et al.* [13] also find that the distribution of receptor types in the mouse olfactory epithelium is highly non-uniform but strain-specific, suggesting a long-term component to the adaptation.

Crucially, in our model the adaptation of receptor distributions for efficient coding occurs before the brain circuitry that decorrelates olfactory inputs. If the input channels were not correlated, efficient coding would predict either equalizing output power across all channels in the transmission-limited case [29, 19], or devoting most resources to those receptors whose responses are most variable in the case in which input noise dominates [15, 30]. This intuition, however, breaks down when there are significant correlations between the responses from different receptors. In this case, the adaptive change in the abundance of a particular receptor type depends critically on the context of the correlated responses of all the receptor types in the population—we refer to this as *context-dependent adaptation*. In the case of olfaction, such correlations are inevitable because 1) the same odorant binds to many different receptors, and 2) odors in the environment are composed of several different odorants, leading to correlations between the concentrations with which these odorants are encountered in natural scenes. We develop the theory of efficient coding to take into account such correlations. The resulting model predicts that receptor abundances and their sensitivity to environment changes should be highly context-dependent, matching the experimental observations [9, 10, 12, 13].

2 Model

2.1 Olfactory response model

Before turning to the specifics of our model, we briefly introduce the anatomy of the olfactory periphery. In vertebrates, axons from olfactory neurons converge in the olfactory bulb on compact structures called glomeruli, where they form synapses with the dendrites of downstream neurons [31]; see Figure 1a. To a good approximation, each glomerulus receives axons from only one type of OSN, and all the OSNs expressing the same receptor type converge onto a small number of glomeruli, on average about 2 in mice to about 16 in humans [32]. A similar architecture can be found in insects [33].

The anatomy shows that in insects and vertebrates, the olfactory information that is passed to the brain can be summarized by the activity at the level of the glomeruli. For the purposes of our model, we will treat this activity in a firing-rate approximation, ignoring the timing of individual spikes. There is evidence that at least in mammals, but perhaps also in insects, timing is important for odor discrimination [34, 35, 36, 37]. This could be incorporated into our model by using the timing of spikes instead of the average firing rate as a measure of receptor activity, but we do not do so here. We will also assume that all neurons of a given type converge onto a single glomerulus (as in Figure 1a). This is because within our model, information transfer only depends on the total number of neurons of a given type, and does not change if their outputs are split over several glomeruli (see Supporting Information).

There is comparatively less known regarding the structure of odor environments. In fact, one of the difficulties specific to the study of the olfactory system when compared to other senses is the lack of a good canonical model for odor space. It is in general difficult to identify the common features shared by

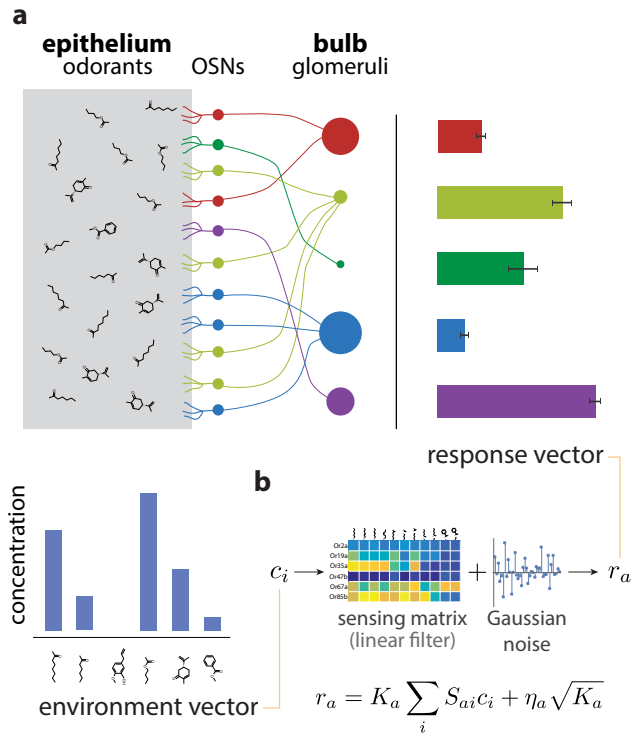

Figure 1: Sketch of the olfactory periphery as described in our model. **(a)** Sketch of vertebrate olfactory anatomy. In insects, the antennae and antennal lobes contain the OSNs and glomeruli, respectively. Different receptor types are represented by different colors. Glomerular responses (bar plot on top right) result from mixtures of odorants in the environment (bar plot on bottom left). The response noise, shown by black error bars, depends on the number of receptors of each type, illustrated in the figure by the size of the corresponding glomerulus. Glomeruli receiving input from a small number of OSNs have higher variability due to receptor noise (*e.g.,* OSN, glomerulus, and activity bar in dark green), while those receiving input from many OSNs have smaller variability. Response magnitudes depend also on the odorants present in the medium and the affinity profile of the receptors (*e.g.,* blue bar is smaller than green bar despite blue glomerulus being larger). **(b)** We approximate glomerular responses using a linear model based on a "sensing matrix" S, perturbed by Gaussian noise η_a. K_a are the multiplicities of each receptor type.

odorants that activate a given receptor type [38, 2], while attempts at defining a notion of distance in olfactory space have had only partial success [39], as have attempts to find reduced-dimensionality representations of odor space [40, 41]. In this work, we simply model the olfactory environment as a vector $\mathbf{c} = \{c_1, \ldots, c_N\}$ of concentrations, where c_i is the concentration of odorant i in the environment (Figure 1). In fact, the mathematical analysis does not depend in any way on this interpretation—it could instead represent a different abstraction, such as the concentrations of classes of molecules clustered based on common chemical traits, or abstract coordinates in a low-dimensional representation of olfactory space.

With this parametrization, the statistics of natural scenes can be summarized by the joint probability distribution $P(c_1, \ldots, c_N)$. This ignores temporal correlations in olfactory cues, which is an approximation that has been used successfully in similar studies in the visual system [42, 30]. We aim here to obtain a tractable model that allows us to build intuition regarding the relation between natural odor statistics and olfactory receptor distributions. For this reason, we model the probability distribution of the environment vector as a multivariate Gaussian with mean $\mathbf{c}_0$ and covariance matrix Γ,

$$\text{environment } P(\mathbf{c}) \sim \mathcal{N}(\mathbf{c}_0, \Gamma)\,. \tag{1}$$

We only need to include in our information maximization procedure those odorants that are likely to be encountered at meaningful concentrations in the typical environment of a given animal. This number N,

though still large, will be much smaller than the total number of possible odorants (which could be in the billions [1]). In our numerical studies the main limitation on the number of odorants comes from the availability of affinity data. We thus take N of order 100, matching the number of odorants available in the receptor response data that we use, 110 in fly [43] and 63 in mammals [44].

In order to find the amount of information that the brain receives about an olfactory scene, we need to model the way in which glomerular responses depend on the odor environment. We assume here a linear model (Figure 1b), in which increasing the concentration of an odorant by a certain factor leads to an increase in the activation of a receptor by the same factor, and the response to odor mixtures is the sum of the activations from each of the components. We define the response of a given glomerulus as simply the sum of the responses from all the olfactory neurons that project to it. These assumptions can be thought of as linearizing the full non-linear responses in the olfactory epithelium around a given operating point. Note that since we model all the responses in a linear way, we make no difference between changes in the number of receptor molecules per neuron, and changes in the number of olfactory neurons of a given type. In general these could have different effects due to nonlinear neuronal responses.

Mathematically, we write

$$r_a = K_a \sum_i S_{ai} c_i + \eta_a \sqrt{K_a}\,, \tag{2}$$

where S_{ai} is the expected response of a sensory neuron expressing receptor type a to a unit concentration of odorant i, and K_a is the number of neurons of type a. The second term models noise, with η_a being the noise for a single OSN. We use a Gaussian approximation for η_a and we normalize the responses by the standard deviation of the noise for a single neuron, so that η_a are drawn from independent standard normal distributions, $\eta_a \sim \mathcal{N}(0,1)$.

2.2 Information maximization

To quantify the amount of information that the response vector $\mathbf{r}$ contains about the environment vector $\mathbf{c}$, we use the mutual information $I(\mathbf{r},\mathbf{c})$ between these two quantities:

$$I(\mathbf{r},\mathbf{c}) = \int d^M r d^N c\, P(\mathbf{r},\mathbf{c}) \cdot \log\left[\frac{P(\mathbf{r}|\mathbf{c})}{P(\mathbf{r})}\right]\,, \tag{3}$$

where $P(\mathbf{r},\mathbf{c})$ is the joint probability distribution over response and concentration vectors, $P(\mathbf{r}|\mathbf{c})$ is the distribution of responses conditioned on the environment, and $P(\mathbf{r})$ is the marginal distribution of the responses alone. Given the assumptions we made, all of these distributions are Gaussian, and the integral can be evaluated analytically (see Supporting Information). The result is

$$I(\mathbf{r},\mathbf{c}) = \frac{1}{2}\,\mathrm{Tr}\log(\mathbb{I} + \mathbb{K}Q)\,, \tag{4}$$

where the *overlap matrix* Q is related to the covariance matrix Γ of odorant concentrations in natural scenes (from eq. (1)),

$$Q = S\Gamma S^T\,, \tag{5}$$

and $\mathbb{K}$ is a diagonal matrix containing the receptor abundances K_a,

$$\mathbb{K} = \mathrm{diag}\big(K_1, K_2, \ldots, K_M\big)\,. \tag{6}$$

In the absence of noise, the overlap matrix Q is equal to the covariance matrix of receptor responses averaged over the ensemble of natural odors. Because of the way in which we normalized the receptor responses, the quantity $\mathbb{K}Q$ thus behaves as a signal-to-noise ratio (SNR), so that eq. (4) is essentially a generalization to multiple, correlated channels of the standard result for a single Gaussian channel, $I = \frac{1}{2}\log(1+\mathrm{SNR}^2)$ [45, 18, 15].

The receptor numbers K_a cannot grow without bound; they are constrained by the fact that the total number of neurons in the olfactory epithelium has to stay within realistic limits. Thus, to find the optimal

distribution of receptor types, we maximize $I(\mathbf{r}, \mathbf{c})$ with respect to $\{K_a\}$, subject to the constraints that: (1) the total number of receptor neurons is fixed; and (2) all neuron numbers are non-negative,

$$\{K_a\} = \arg\max I(\mathbf{r}, \mathbf{c}) \,, \tag{7a}$$

$$\text{subject to} \begin{cases} K_{\text{tot}} = \sum_a K_a = \text{const}, \\ K_a \geq 0 \,. \end{cases} \tag{7b}$$

The optimization can be performed analytically using the Karush-Kuhn-Tucker (KKT) conditions [46] (see Supporting Information), but in practice it is more convenient to use numerical optimization.

It is worth noting that, due to the fact that mutual information is invariant under invertible transformations of concentrations and responses, our results apply equally well to cases in which the response from eq. (2) is generalized to include some nonlinearities (see Discussion).

3 Results

Our model predicts the optimal distribution of receptor types given receptor affinities, the statistics of natural odors, and the size of the olfactory epithelium. In the following sections, we analyze how the model results depend on these factors, and how they compare to experimental observations.

3.1 The total number of sensory neurons controls the diversity of olfactory receptors in the epithelium

All receptors are equally represented in large OSN populations In our model, the effect of receptor noise can be diminished by averaging over the responses from many sensory neurons. In the limit in which the total number of neurons is allowed to grow very large, $K_{\text{tot}} \to \infty$, the signal-to-noise ratio (SNR) becomes very large, and the averaged glomerular responses become effectively noiseless (see eq. (2)). When this happens, the optimization from eq. (7) can be solved analytically (see Supporting Information), and we find that the optimal receptor distribution is given by

$$K_a = \frac{K_{\text{tot}}}{M} - (A_{aa} - \bar{A}) + \mathcal{O}(A^2/K^2) \,, \tag{8}$$

where A is the inverse of the overlap matrix defined in eq. (5), $A = Q^{-1}$, and $\bar{A} = \sum A_{aa}/M$ is the average diagonal element of this matrix. In other words, the receptor distribution is essentially uniform, with each receptor type being expressed in a roughly equal fraction of the total population of sensory neurons, with small differences related to the diagonal elements of the inverse overlap matrix A (see Figure 2a). It turns out also that the information maximum in this regime is very shallow. This is because only a change in receptor numbers of order K_{tot}/M can have a significant effect on the noise level for the activity of each glomerulus. Put another way, when the receptor numbers K_a are very large, the responses are effectively noiseless, and in the noiseless case the number of receptors of each type has no effect on the reliability of the responses, and thus it has no effect on information transfer. The approximation in eq. (8) holds as long as the receptor abundances K_a are much larger than the elements of the inverse overlap matrix A, and it breaks down otherwise (see the points on the right in Figure 2f).

Smaller OSN populations have less diverse receptors When the number of neurons is very small, receptor noise can overwhelm the response to the environment. In this case, we find that the best strategy is to focus all the available neurons on a single receptor type, thus reducing noise as much as possible (Figure 2b). The receptor type that yields the highest contribution to the information turns out to be the one whose response is most variable in natural scenes (that is, the one that corresponds to the largest value of Q_{aa}; see Supporting Information for a derivation). This is reminiscent of a result in vision where the variance of a stimulus predicted its perceptual salience [30]. As the total number of neurons increases, the added benefit from lowering the noise for a single receptor type diminishes, and at some critical value it becomes more advantageous in terms of maximizing information to start populating a second receptor type (Figure 2b).

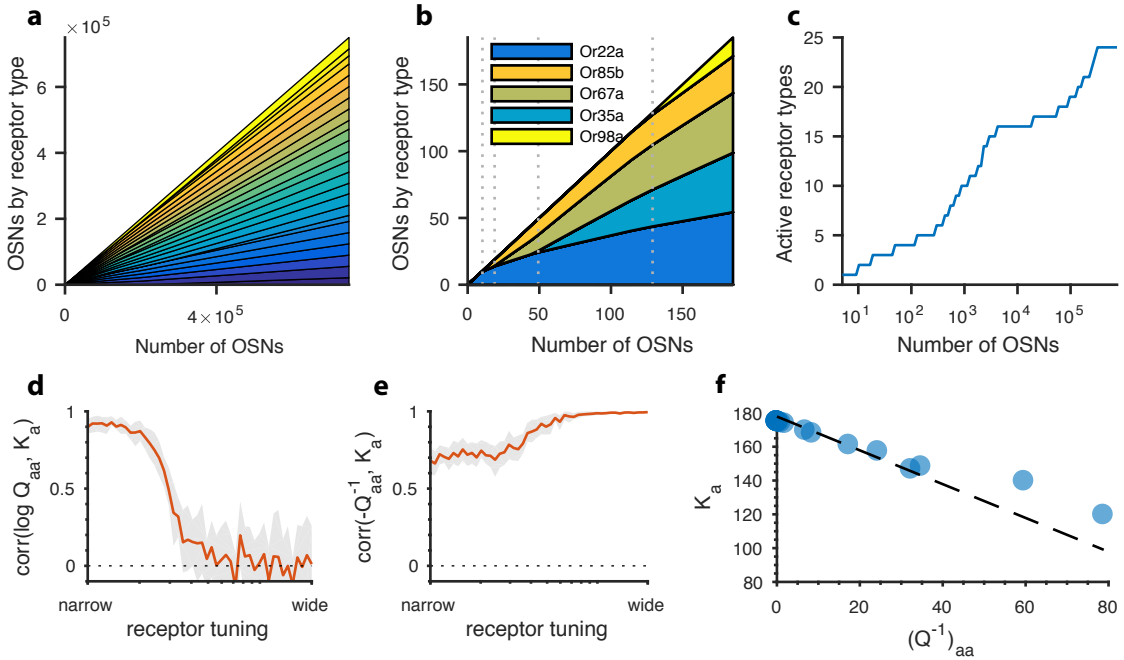

Figure 2: Building an intuition for the results from our model. **(a)** When the total number of neurons, K_{tot}, is large, the optimal distribution of receptors is approximately uniform, with each receptor type taking up an equal fraction of the total (represented here by strips of different colors). **(b)** When the number of neurons K_{tot} is low, only a small number of receptor types are expressed when information is maximized. **(c)** New receptor types become expressed in a series of step transitions as the total number of neurons increases. In panels **a**–**c**, results were obtained using a sensing matrix based on measurements in the fly [43] and environmental odor statistics following a random correlation matrix (see Supporting Information for details). However, the qualitative aspects are generic. **(d)** Correlation between the abundance of a given receptor type, K_a, and the logarithm of the variance with which it is activated in olfactory scenes, $\log Q_{aa}$, shown here as a function of the tuning of the receptors. For every position along the x-axis, sensing matrices with a fixed receptor tuning width were generated from a random ensemble. Roughly-speaking, the tuning width on the x-axis indicates what fraction of all odorants elicit a strong response for the receptors; in the figure, this ranges from 0.01 to 0.2. See Supporting Information for details. When each receptor responds strongly to only a small number of odorants, response variance is a good predictor of abundance, while this is no longer true for wide tuning. **(e)** Receptor abundances correlate well with the diagonal elements of the inverse overlap matrix, $(Q^{-1})_{aa}$, for all tuning widths, with somewhat lower correlations at narrow tuning. In **d** and **e**, the red line is the mean obtained from 24 simulations, each performed using a different sensing matrix, and the light gray area shows the interval between the 20th and 80th percentiles of results. **(f)** Example showing the dependence between receptor abundances and the diagonal elements of the inverse overlap matrix in a simulation using a wide-tuning sensing matrix and an intermediate SNR. The dashed line corresponds to the approximation from eq. (8).

In natural olfactory systems, the distribution of receptor types is highly non-uniform, and is more conserved for individuals of the same species than between species [13]. This matches the results from our model in an intermediate SNR range, where noise is significant but does not overwhelm the olfactory signal. This is consistent with the idea that living systems would conserve resources and set the number of OSNs (and, thus, the SNR) close to the minimum necessary.

Receptor diversity grows with OSN population size More generally, our model predicts that the number of receptor types that are expressed should increase monotonically with the total number of sensory neurons, in a series of step transitions (see Figure 2c). This provides an interesting prediction that could be

tested by looking at the relation between the size of the olfactory epithelium and the number of functional receptor genes in various species. A caveat here is that we are assuming the sensing matrix S and environmental statistics Γ stay the same while varying only the total number of neurons K_{tot}. This restricts an empirical test of this prediction to groups of closely-related species.

3.2 Receptor abundances are highly context-dependent

By maximizing the mutual information in eq. (4) while keeping the total number of receptors $K_{\text{tot}} = \sum_a K_a$ constant, we can predict the optimal receptor distribution K_a given the sensing matrix S and the statistics of environmental odors. The optimization exhibits a rich set of behaviors, in accordance with experimental evidence, where receptor abundances can either increase or decrease upon increased exposure to ligands [9, 10, 12, 13]. We sought an intuitive way to understand this result from our model.

A simple observation is that the average concentration vector $\mathbf{c}_0$ has no impact on the optimal distribution. This is because it corresponds to odors that are always present and thus offer no new information about the environment, and is consistent with experimental observations [13]. Thus, the environmental statistics affect the optimal receptor distribution only through the covariance matrix Γ.

It is intuitively clear that, at least in the limit in which receptor responses are uncorrelated, receptors whose activations fluctuate extensively in natural olfactory scenes provide the brain with a lot of information about the odor environment (assuming noise is negligible). In contrast, receptors that are almost silent or are constantly active at about the same rate are not very informative. It thus seems advantageous to increase the number of neurons expressing receptors of the first kind, and not focus many resources on receptors of the second kind [30]. In terms of our model, the variances of the glomerular responses in natural scenes are given (in the absence of noise) by the diagonal elements of the overlap matrix Q defined in eq. (5), so our intuition would dictate that the number of receptors of type a grows with the variance corresponding to that receptor type, $K_a \sim Q_{aa}$.

Even when there are correlations between receptor responses, the intuition above applies in the very low SNR regime, when only one receptor type is active. As we saw in the previous section, in that case, the receptor type that should be active to maximize information is indeed the one with the largest variance Q_{aa}. The intuition also holds when the sensing matrix is narrowly-tuned: if each receptor type responds to only a small number of odorants, the abundances of OSNs of each type correlate well with the amount of variability that the corresponding receptors experience in natural scenes (narrow-tuning side of Figure 2d). Thus in all these cases, the abundance of a receptor type is directly correlated to the variability of its responses in the environment, a result that coincides with conventional intuition.

The biological setting, however, is better described in our model by a regime with widely-tuned sensing matrices [43], and an intermediate SNR level in which noise is important, but does not dominate the responses of most receptors. To see how the tuning width affects the results from the model, we generated sensing matrices with varying tuning width by changing the number of odorants that exhibit strong responses for each receptor (detailed Methods in Supporting Information). We found that as each receptor type starts responding to more and more odorants, the *correlation structure* of the receptor responses becomes important in determining the optimal receptor distribution, and the intuition based on only the response variances no longer holds (wide-tuning side of Figure 2d). In other words the optimal abundance of a receptor type depends not just on its activity level, but also on the correlated activity levels of all the other receptor types. This mimics the context-dependence seen in experiments.

Above, we showed analytically in eq. (8) that in the high SNR limit the optimal receptor distribution is anti-correlated with the diagonal elements of the *inverse* of the overlap matrix, $A = Q^{-1}$, rather than with the variance of the receptor response (*i.e.,* diagonal elements of Q itself). In Supporting Information we show that this occurs because receptors that have a high $(Q^{-1})_{aa}$ either do not provide much olfactory information because their responses do not fluctuate much; or they provide information that is largely redundant given all the others. Either way, they should therefore not be very abundant in the optimal distribution. In contrast, receptors with low $(Q^{-1})_{aa}$ contain a lot of independent olfactory information, and so they are predicted to be abundant. In fact, this inverse relation remains a good approximation even in the broadly-tuned and intermediate SNR regimes that are biologically relevant (Figure 2d-f). Because of the matrix inversion, the optimal distribution in these regimes is affected by the full covariance structure of the receptor responses. This leads to a complex context-dependence in the optimal abundance of receptor types, as observed in

experiments.

3.3 Dependence on the environment

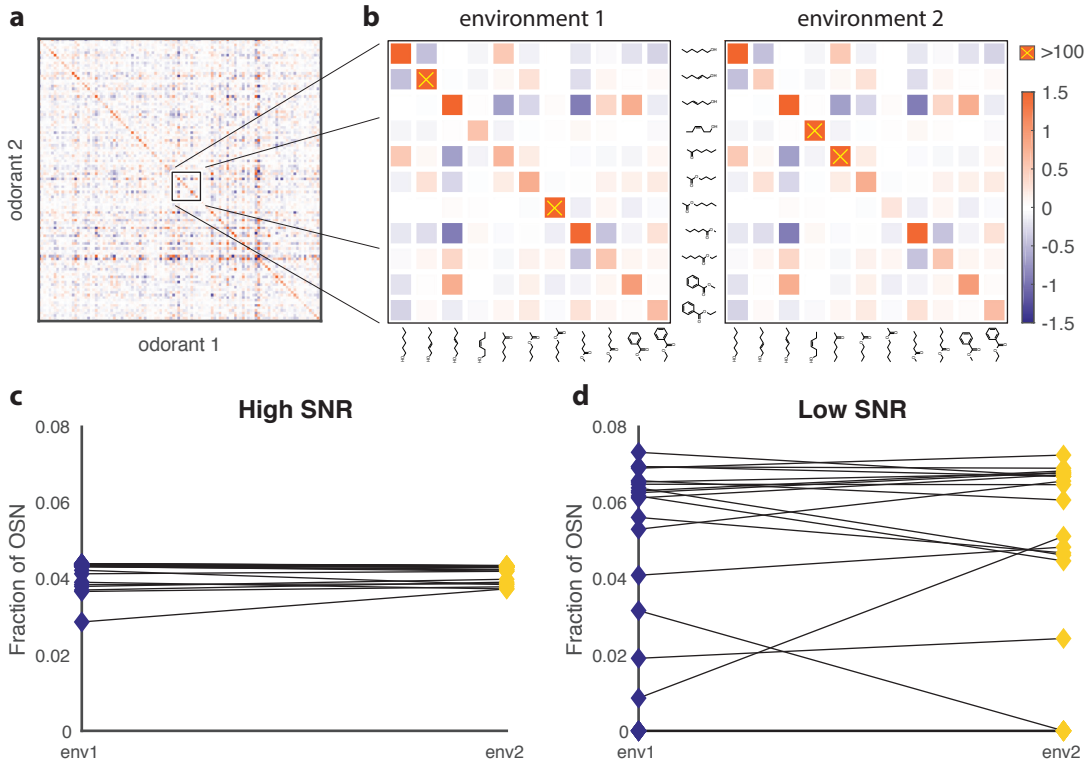

Figure 3: Effect of changing environment on the optimal receptor distribution in our model. **(a)** An example of an environment covariance matrix used in our model. We use an algorithm that generates random covariance matrices with a tunable amount of cross-correlation (see Supporting Information for details). The variances are drawn from a lognormal distribution. **(b)** Close-ups showing some of the differences between the two environments used to generate the results from **c** and **d**. The two different covariance matrices are obtained by starting with the matrix from **a** and adding a large amount of variance to two different sets of 10 odorants (out of 110). The altered odorants are identified by yellow crosses; their corresponding variances go above the color scale on the plots by more than 60 times. **(c)** Change in receptor distribution when going from environment 1 to environment 2, in conditions where the total number of receptor neurons K_{tot} is large (the SNR is high). The blue diamonds on the left correspond to the optimal OSN fractions per receptor type in the first environment, while the yellow diamonds on the right correspond to the second environment. In this high-SNR regime, the effect of the environment is small, because in both environments the optimal receptor distribution is close to uniform. **(d)** When the total number of neurons K_{tot} is small (the SNR is low), changing the environment can have a dramatic effect on optimal receptor abundances, with some receptors that are almost vanishing in one setting becoming highly abundant in the other, and *vice versa*.

Environmental changes lead to complex patterns of receptor abundance changes To get some intuition for the dependence on the environment in our model, we used a sensing matrix based on measurements in the fly [43], and compared the predicted receptor distributions in two different environments, at two different noise levels (or, equivalently, two different values for the total number of OSNs K_{tot}); see Figure 3.

Unfortunately, there are no measurements available for the distributions of natural odors. As such, we have little information to guide our choice for the statistical structure of odorant concentrations, modeled here by a Gaussian $\mathcal{N}(\mathbf{c}_0, \Gamma)$. To get a qualitative understanding of the efficient coding of olfactory scenes, we therefore took the environment as having a random covariance matrix (see Figure 3a for an example;

see Supporting Information for details). Starting with a base environment, we then generated two different environments by adding a large amount of variance to 10 odorants in environment 1, and to 10 different odorants in environment 2 (Figure 3b).

Our results show that, when the number of olfactory sensory neurons K_{tot} is large, and thus the signal-to-noise ratio is high, the change in odor statistics has little effect on the distribution of receptors (Figure 3c). This is because at high SNR, the distribution is essentially uniform regardless of environment, as explained earlier. When the number of neurons is smaller (or, equivalently, the signal to noise ratio is in a low or intermediate regime), the change in environment has a significant effect on the receptor distribution, with some receptor types becoming more abundant, others becoming less abundant, and yet others not changing much (see Figure 3d). This mimics the kinds of complex effects seen in experiments in mammals [8, 9, 10, 11, 12, 13].

Strikingly, and consistently with the findings in [8, 9, 10, 11, 12, 13], whether a certain receptor abundance goes up or down as a result of a given change in environment is hard to guess, as it is a global effect that depends on how the change affects the activation of all receptor types, as well as the correlations between these activations. As a rough approximation, the change in abundance ΔK_a is related to the change in the corresponding element of the inverse overlap matrix, $\Delta(Q^{-1})_{aa}$. However, this estimate does not work as well when receptors are narrowly-tuned, where the approximation $K_a \approx C - (Q^{-1})_{aa}$ for some constant C is less accurate.

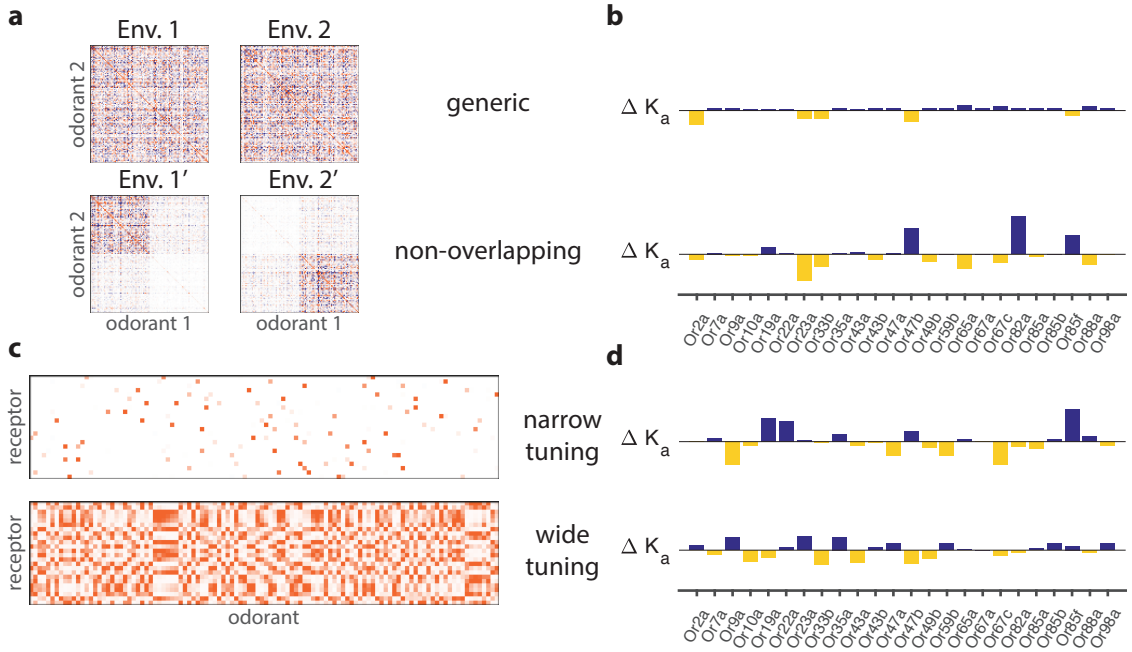

Figure 4: The effect of a change in environmental statistics on the optimal receptor distribution as a function of overlap in the odor content of the two environments, and the tuning properties of the olfactory receptors. **(a)** Random environment covariance matrices used in our simulations (red is positive [co-]variance, blue is negative, white is zero). The environments on the top span a similar set of odors, while those on the bottom contain largely non-overlapping sets of odors. **(b)** The change in receptor distribution tends to be small when both environments span a similar set of odors, even when the detailed statistics are very different (top). The change is much larger when the two environments contain different odors (bottom). The results in **a** and **b** are based on receptor affinity data from the fly [43] **(c)** Sensing matrices we used in our simulations. On top, a sensing matrix with narrowly-tuned receptors, which respond to small numbers of odorants (tuning parameter of 0.05—see Supporting Information). On the bottom, a sensing matrix with broadly-tuned receptors (tuning parameter of 0.8—see Supporting Information). **(d)** Narrowly-tuned receptors result in optimal receptor distributions that are more sensitive to changes in environment (top). Broadly-tuned receptors tend to average out differences in environmental statistics of odors (bottom).

Changing odor identities has a larger effect on receptor distributions than changing concentrations In the comparison above, the two environment covariance matrices differed in a small number of positions by a large amount. In contrast, Figure 4b shows what happens if we instead compare environments with two different randomly-generated covariance matrices, each generated in the same way as the background environment in Figure 3a. The resulting environmental covariance matrices (Figure 4a, top) are very different in detail (for example, the correlation coefficient between their entries is close to zero), although they look similar by eye. Nevertheless, the corresponding change in receptor distribution is very small, with just a few receptor types experiencing larger changes in abundance (Figure 4b, top).

If instead we engineer two environments that are almost non-overlapping, meaning that each odorant is either common in environment 1, or in environment 2, but not in both (Figure 4a, bottom), the changes in receptor abundances become much larger, with some receptors going from highly abundant to vanishing from the population, while others going in the opposite direction, from not being expressed at all, to high abundance (Figure 4b, bottom). This shows that the particular way in which the environment changes, and not only the magnitude of the change, can alter the effect on the receptor distribution. In biological terms, we would indeed expect animals that experience very different kinds of odors to have more striking differences in their receptor repertoires than those that merely experience the same odors with different frequencies. Our results quantify the expected difference.

The magnitude of the effect of environmental changes on the optimal olfactory receptor distribution is partly controlled by the tuning of the olfactory receptors (Figure 4c). If receptors are narrowly-tuned, with each type responding to a small number of odorants, changes in environment tend to have more drastic effects on the receptor distribution than when the receptors are broadly-tuned (Figure 4d), an effect that could be experimentally tested.

Model predictions qualitatively match experiments Our study opens the exciting possibility of a causal test of the hypothesis of efficient coding in sensory systems, where a perturbation in the odor environment could lead to predictable adaptations of the olfactory receptor distribution during the lifetime of an individual. This does not happen in insects, but it can happen in mammals, since their receptor neurons regularly undergo apoptosis and are replaced.

A recent study demonstrated that reproducible changes in olfactory receptor distributions of the sort that we predict can occur in mice [13]. Specifically, Ibarra-Soria *et al.* [13] raised two groups of mice in similar conditions, exposing one group to a mixture of four odorants (acetophenone, eugenol, heptanal, and R-carvone) either continuously or intermittently (by adding the mixture to their water supply). Continuous exposure to the odorants had no effect on the receptor distribution, in agreement with the predictions of our model, in which the average concentration vector $\mathbf{c}_0$ drops out of the mutual information calculations. In contrast, intermittent exposure did lead to systematic changes in the receptor distribution (see Figure 5a).

We used our model to run an experiment similar to that of Ibarra-Soria *et al.* [13] *in silico*. Using a sensing matrix based on odor response curves for mouse and human receptors [44], we calculated the predicted change in receptor abundances between two different environments with random covariance matrices. The results (see Figure 5b) show that most receptor abundances do not change much, especially for those receptors that were very abundant to start with; there is more change in the middle of the abundance range; while the abundances of rare receptors change significantly, but are highly sensitive to small perturbations in the environment. The sensitivity to perturbations was estimated by running the simulation 24 times, each time modifying the covariance matrices for the initial and final environments. This was done by adding a small amount of Gaussian random noise to the square roots of these covariance matrices (see Supporting Information).

The simulation results qualitatively match the experimental results (see Figure 5a), where we see the same pattern of the largest reproducible changes occurring for receptors with intermediate abundances. In principle this comparison could be made quantitative by using the same perturbation in our simulations as that used in the experiments from [13]. This is not yet possible for several reasons. Most importantly, sensing data is missing for one of the four odorants used in the experiments (eugenol). Furthermore, affinity data is only available for a small fraction of receptor types (52 mouse and 10 human receptors, compared to more than 1000 total receptors in the mouse), and a small number of odorants (63, although even for these 62×63 pairs, most responses were below the measurement threshold; see Supporting Information). Since the reorganization of the receptor distribution is a global phenomenon that depends on the responses from all glomeruli, this makes it hard to interpret any results obtained with such a small subset of receptors. Precise

predictions are also made difficult because the statistics of natural odors to which the mice are exposed are unknown, and even the statistics with which the mice encounter the odorant mixture used in the experiment are hard to guess. All these issues make it impossible to produce specific predictions at this point, although many of them can be addressed in future experiments.

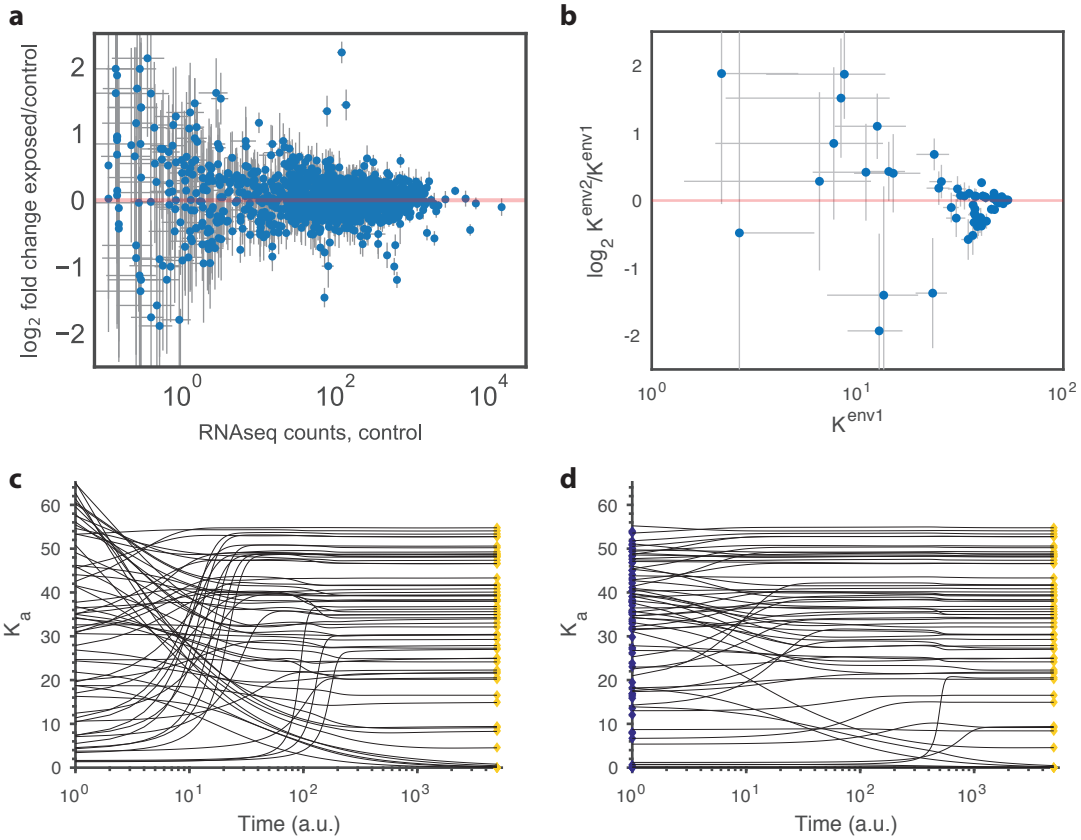

Figure 5: Qualitative comparison between experiment and theory regarding the changes in receptor distribution that occur with a change in environment; and an example of convergence in our dynamical model. **(a)** Reproduced using the raw data from [13], this shows the experimental data for the log-ratio between the receptor abundances in the mouse epithelium in the test environment (where four odorants were added to the water supply) and those in the control environment, plotted against the values in the control conditions (on a log scale). The error bars show standard deviation across six individuals. Compared to Figure 5B in [13], this plot does not use a Bayesian estimation technique that shrinks ratios of abundances of rare receptors towards 1 (personal communication with Professor Darren Logan, June 2017). **(b)** A similar plot produced in our model using mouse and human receptor response curves [44]. The error bars show the range of variation found in the optimal receptor distribution when slightly perturbing the initial and final environments (see the text). The simulation includes 62 receptor types for which response curves were measured [44], compared to 1115 receptor types assayed in [13]. **(c)** Example convergence curves in our dynamical model showing how the optimal receptor distribution (yellow diamonds) is reached from a random initial distribution of receptors. Note that the time axis is logarithmic. **(d)** Convergence curves when starting close to the optimal distribution from one environment (blue diamonds) but optimizing for another. A small, random deviation from the optimal receptor abundance in the initial environment was added to avoid the simulation getting trapped in a local optimum.

3.4 First steps towards a dynamical model in mammals

We have explored the structure of olfactory receptor distributions that code odors efficiently, *i.e.,* are adapted to maximize the amount of odor information that the brain gets about the environment. The full solution to the corresponding optimization problem, eq. (7), depends in a complicated nonlinear way on the receptor affinities S and natural distribution of odorants Γ. The distribution of olfactory receptors in the mammalian epithelium, however, must arise dynamically, from the pattern of apoptosis and neurogenesis [47]. It would thus be useful to have a dynamical implementation of our model. In the efficient coding paradigm that we propose, the receptor distribution is intimately related to the statistics of natural odors, so that the life cycle of neurons in a dynamical model implementation would have to depend on olfactory experience. And indeed, such modulation of OSN lifetime by exposure to odors has been observed experimentally [9, 10, 12] and could, for example, be mediated by feedback from the bulb [8].

To obtain a dynamical version of our model, we started with a gradient ascent argument algorithm and modified it slightly to impose the constraints from eq. (7b) (details in Supporting Information). This gives

$$\frac{dK_a}{dt} = \alpha \left\{ K_a - \lambda K_a^2 - (R^{-1})_{aa} K_a^2 \right\} , \tag{9}$$

where α is a learning rate and R is the covariance matrix of glomerular responses,

$$R_{ab} = \langle r_a r_b \rangle - \langle r_a \rangle \langle r_b \rangle , \tag{10}$$

with the angle brackets denoting ensemble averaging over natural odors and averaging over receptor noise. In the absence of the experience-related term $(R^{-1})_{aa}$, the dynamics from eq. (9) would be simply logistic growth: the population of OSNs of type a would initially grow at a rate α, but would saturate when $K_a = 1/\lambda$ because of the population-dependent death rate λK_a. In other words, the quantity M/λ sets the asymptotic value for the total population of sensory neurons, $K_{\text{tot}} \to M/\lambda$, with M being the number of receptor types.

Because of the last term in eq. (9), the death rate in our model is influenced by olfactory experience in a receptor-dependent way. In contrast, the birth rate is not experience-dependent, and is the same for all OSN types. And indeed, in experiments, the odor environment is seen to have little effect on receptor choice, but does modulate the rate of apoptosis in the olfactory epithelium [9]. A complete understanding of the mechanisms affecting the lifetime of olfactory sensory neurons and how these are regulated is not yet available, so experiments do not yet constrain the way in which neuronal death depends on olfactory experience. Our results suggest that, if this dependence is appropriately anti-correlated with the inverse response covariance matrix, then the receptor distribution in the epithelium can converge to achieve optimal information transfer to the brain.

The elements of the response covariance matrix R_{ab} could be estimated by taking temporal averages of products of glomerular activations, which could take advantage of lateral connections between glomeruli [48]. Performing the inverse necessary for our model is more intricate, but this could be done at the level of the bulb and fed back to the epithelium through mechanisms that have been observed in experiments [8]. We leave the development of a fully mechanistic model for the adaptation of olfactory receptor populations for future work.

Within our model, Figure 5c shows example convergence curves when starting from a random initial distribution. The sensing matrix used here is based on mammalian data [44] and the environment covariance matrix is generated using the random procedure mentioned earlier (and described in more detail in the Supporting Information). We see that some receptor types take much longer than others to converge (the time axis is logarithmic, which helps visualize the whole range of convergence behaviors). Roughly-speaking, convergence is slower when the final receptor abundance is small, which is related to the fact that the rate of change dK_a/dt in eq. (9) vanishes in the limit $K_a \to 0$.

In Figure 5d, we show the convergence to the same final state, but this time starting from a distribution that is not random, but was optimized for a different environment. The initial and final environments are the same as those used in the previous section to compare the simulations to experimental findings, Figure 5b. Interestingly, many receptor types actually take longer to converge in this case compared to the random starting point, showing that getting trapped in local optima is a potential danger. This can be alleviated by adding a small amount of stochasticity to the dynamics, which in realistic situations would enter naturally since the response covariance matrix R would have to be estimated based on stochastic odor encounters and

noisy receptor readings. In fact, in Figure 5d, we needed to add a small amount of noise (corresponding to $\pm 0.05 K_{\text{tot}}$) to the initial distribution to improve convergence and avoid getting trapped.

4 Discussion

We built a model for the distribution of receptor types in the olfactory epithelium that is based on efficient coding, and assumes that the abundances of different receptor types are adapted to the statistics of natural odors in a way that maximizes the amount of information conveyed to the brain by glomerular responses. This model predicts a non-uniform distribution of receptor types in the olfactory epithelium, as well as reproducible changes in the receptor distribution as a result of perturbations in the odor environment. In contrast to other efficient coding applications, our model operates in a regime in which there are significant correlations between the inputs because the adaptation of receptor abundances occurs upstream of the brain circuitry that can decorrelate olfactory responses. In this regime, receptor abundances depend on the full correlation structure of the inputs, leading to predictions that are context-dependent in the sense that whether the abundance of a specific receptor goes up or down due to a shift in the environment cannot be easily guessed based on the responses of that receptor alone. All of these striking phenomena have been observed in recent experiments, and our model provides a potential conceptual framework for understanding the data.

In our framework, the sensitivity of the receptor distribution to changes in odor statistics is affected by the tuning of the olfactory receptors, with narrowly-tuned receptors being more readily affected by such changes than broadly-tuned ones. The model also predicts that environments that differ in the identity of the odors that are present will lead to larger differences in optimal receptor distribution than environments that differ only in the statistics with which these odors are encountered. Another prediction is that there is a monotonic relationship between the number of receptor types found in the epithelium and the total number of olfactory sensory neurons. All of these predictions can be tested in future experiments.

While the model agrees with experimental data in its qualitative predictions, a quantitative comparison is not yet possible due to the scarcity of experimental constraints on some of the parameters. More complete surveys of response curves of olfactory receptors to larger panels of odorants in more organisms would help to fix the structure of odor-receptor interactions that is necessary for our model. More high-throughput measurements of the distribution of receptor types in the olfactory epithelium, as in [13], would enable precise tests of the predictions. However, the biggest missing piece at this point is a knowledge of the statistics of natural odors. Perhaps imaging studies focusing on glomeruli in behaving animals could provide a novel way to make such measurements. Or perhaps a mix of theory and experiment could provide a way to estimate naturalistic odor statistics even if these are not precisely matched to any particular environment.

Our work can be extended in several ways, with the caveat that each extension can introduce additional parameters, requiring more experimental data to fix accurately. For instance, OSN responses do not depend linearly on odorant concentrations, but respond in more complex, nonlinear ways. Some of these nonlinearities actually do not affect the results from our model, due to invariances of the mutual information. Specifically, our results would not change if the concentration vector was first passed through an invertible nonlinearity, then mixed according to the sensing matrix, scaled according to the receptor numbers and perturbed by noise, and finally passed through another invertible nonlinearity. These transformations could, however, make it harder to decode the processed information, for instance if the nonlinearities were close to singular. This means that the fundamental assumption that our model is making is not one of linearity, but rather that the noise appears only at the receptor level. In particular, it is assumed that downstream processing of the signal does not suffer from noise or resolution problems.[1] Thus generalizing the model to include nonlinear responses is equivalent to including noise beyond the receptor level.

It is also possible that the mutual information is not the best quantity to maximize [49]. For instance, the importance of a given glomerular response to an animal might be related not only to how much information this gives about the odor environment, but might be modulated by a value assignment. Both theoretical and experimental work is needed to figure out how and if the adaptation of olfactory receptor distributions depends on value. On the natural statistics side, the distribution of odorants might be more appropriately modeled using a Gaussian mixture instead of a normal distribution. This would imply the existence of many odor objects, each of which would be modeled by a Gaussian distribution with a certain concentration profile,

[1] We thank David Zwicker for illuminating discussions regarding this point.

and would more closely approximate the sparse nature of olfactory scenes [25]. All of these extensions we leave for future work.

One exciting possibility suggested by our model is a way to perform a first causal test of the efficient coding hypothesis for sensory coding. Given sufficiently-detailed information regarding receptor affinities and natural odor statistics, experiments could be designed that perturb the environment in specified ways, and then measure the change in olfactory receptor distribution. This could then be compared to the theoretically-predicted changes to provide a strong test of efficient coding ideas. This is in contrast to previous applications of the efficient coding hypothesis in vision and audition, which provided elegant *post-hoc* explanations for observed neural receptive fields but lacked an avenue for testing causality [16, 17, 18, 19, 20, 21, 22, 50, 42, 51, 30, 52, 53].

Acknowledgments

We would like to thank Joel Mainland and David Zwicker for helpful discussions, and Elissa Hallem, Joel Mainland, and Darren Logan for olfactory receptor affinity data. During the completion of this project, VB was supported by Simons Foundation Mathematical Modeling in Living Systems grant 400425 and by the Aspen Center for Physics NSF grant PHY-160761. TT was supported by the Swartz Foundation.

Materials and methods

The code that we used to generate all the results and figures in the paper is available on GitHub, at `https://github.com/ttesileanu/OlfactoryReceptorDistribution`.

References

[1] Chung Wen Yu et al. "Drawing the border of olfactory space". In: *Chemical Senses* 40.7 (2015), pp. 565–565.

[2] Bettina Malnic et al. "Combinatorial receptor codes for odors". In: *Cell* 96.5 (1999), pp. 713–23.

[3] Linda Buck and Richard Axel. "A novel multigene family may encode odorant receptors: A molecular basis for odor recognition". In: *Cell* 65.1 (1991), pp. 175–187.

[4] Andrew Chess et al. "Allelic inactivation regulates olfactory receptor gene expression". In: *Cell* 78.5 (1994), pp. 823–834.

[5] Longzhi Tan, Qian Li, and X Sunney Xie. "Olfactory sensory neurons transiently express multiple olfactory receptors during development". In: *Molecular systems biology* 11.12 (2015), p. 844.

[6] Christine Missbach et al. "Evolution of insect olfactory receptors". In: *eLife* 2014.3 (2014), e02115.

[7] G. A. Monti Graziadei and P. P. C. Graziadei. "Neurogenesis and neuron regeneration in the olfactory system of mammals. II. Degeneration and reconstitution of the olfactory sensory neurons after axotomy". In: *Journal of Neurocytology* 8.2 (1979), pp. 197–213.

[8] James E. Schwob, Karen E. Mieleszko Szumowski, and Audrey A. Stasky. "Olfactory sensory neurons are trophically dependent on the olfactory bulb for their prolonged survival". In: *The Journal of Neuroscience* 12.10 (1992), pp. 3896–3919.

[9] Stephen W. Santoro and Catherine Dulac. "The activity-dependent histone variant H2BE modulates the life span of olfactory neurons". In: *eLife* 2012.1 (2012), pp. 1–32.

[10] Shaohua Zhao et al. "Activity-Dependent Modulation of Odorant Receptor Gene Expression in the Mouse Olfactory Epithelium". In: *PLoS ONE* 8.7 (2013), e69862.

[11] Brian G. Dias and Kerry J. Ressler. "Parental olfactory experience influences behavior and neural structure in subsequent generations". In: *Nature neuroscience* 17.1 (2014), pp. 89–96. arXiv: `arXiv:1011.1669v3`.

[12] Hervé Cadiou et al. "Postnatal Odorant Exposure Induces Peripheral Olfactory Plasticity at the Cellular Level". In: *Journal of Neuroscience* 34.14 (2014), pp. 4857–4870.

[13] Ximena Ibarra-Soria et al. "Variation in olfactory neuron repertoires is genetically controlled and environmentally modulated". In: *eLife* 6 (2017), e21476.

[14] Horace B. Barlow. "Possible principles underlying the transformations of sensory messages". In: *Sensory Communication* (1961), pp. 217–234.

[15] Johannes H. van Hateren. "A theory of maximizing sensory information". In: *Biological Cybernetics* 68.1 (1992), pp. 23–29.

[16] Simon Laughlin. "A Simple Coding Procedure Enhances a Neuron's Information Capacity". In: *Z. Naturforsch.* 36.c (1981), pp. 910–912.

[17] Joseph J. Atick and A. Norman Redlich. "Towards a Theory of Early Visual Processing". In: *Neural Computation* 2 (1990), pp. 308–320.

[18] Johannes H. van Hateren. "Theoretical predictions of spatiotemporal receptive fields of fly LMCs, and experimental validation". In: *Journal of Comparative Physiology A* 171 (1992), pp. 157–170.

[19] Bruno A. Olshausen and David J. Field. "Emergence of simple-cell receptive field properties by learning a sparse code for natural images". In: *Nature* 381.June (1996), pp. 607–609.

[20] Eero P. Simoncelli and Bruno A. Olshausen. "Natural image statistics and neural representation". In: *Annual Review of Neuroscience* 24 (2001), pp. 1193–1216.

[21] Adrienne L. Fairhall, Geoffrey D. Lewen, and William Bialek. "Efficiency and ambiguity in an adaptive neural code". In: *Nature* 412.August (2001), pp. 787–792.

[22] Michael S. Lewicki. "Efficient coding of natural sounds". In: *Nature neuroscience* 5.4 (2002), pp. 356–363.

[23] Charles F. Stevens. "What the fly's nose tells the fly's brain". In: *PNAS* 112.30 (2015), pp. 9460–5.

[24] Yilun Zhang and Tatyana O. Sharpee. "A Robust Feedforward Model of the Olfactory System". In: *PLoS computational biology* 12.4 (2016), e1004850.

[25] Kamesh Krishnamurthy et al. "Disorder and the neural representation of complex odors: smelling in the real world". In: *arXiv* (2017). arXiv: `1707.01962`.

[26] Andreas Keller and Leslie B. Vosshall. "Influence of odorant receptor repertoire on odor perception in humans and fruit flies". In: *Proceedings of the National Academy of Sciences of the United States of America* 104.13 (2007), pp. 5614–9.

[27] Carolyn S. McBride et al. "Evolution of mosquito preference for humans linked to an odorant receptor". In: *Nature* 515.7526 (2014), pp. 222–227.

[28] David Zwicker, Arvind Murugan, and Michael P. Brenner. "Receptor arrays optimized for natural odor statistics". In: *Proceedings of the National Academy of Sciences* 113.20 (2016), pp. 5570–5575. arXiv: `1602.02974`.

[29] M. V. Srinivasan, S. B. Laughlin, and A. Dubs. "Predictive Coding: A Fresh View of Inhibition in the Retina". In: *Proceedings of the Royal Society B: Biological Sciences* 216.1205 (1982), pp. 427–459.

[30] Ann M. Hermundstad et al. "Variance predicts salience in central sensory processing". In: *eLife* 10.7554 (2014), e03722.

[31] John G. Hildebrand and Gordon M. Shepherd. "Mechanisms of olfactory discrimination: converging evidence for common principles across phyla". In: *Annual Review of Neuroscience* 20 (1997), pp. 595–631.

[32] Alison Maresh et al. "Principles of glomerular organization in the human olfactory bulb - Implications for odor processing". In: *PLoS ONE* 3.7 (2008).

[33] Leslie B. Vosshall, Allan M. Wong, and Richard Axel. "An olfactory sensory map in the fly brain". In: *Cell* 102.2 (2000), pp. 147–159.

[34] Arbora Resulaj and Dmitry Rinberg. "Novel Behavioral Paradigm Reveals Lower Temporal Limits on Mouse Olfactory Decisions". In: *Journal of Neuroscience* 35.33 (2015), pp. 11667–11673.

[35] Shamik DasGupta and Scott Waddell. "Learned odor discrimination in Drosophila without distinct combinatorial maps in the antennal lobe". In: *Current Biology* 18.21 (2008), pp. 1668–1674.

[36] Michael Wehr and Gilles Laurent. "Odour encoding by temporal sequences of firing in oscillating neural assemblies". In: *Nature* 384.November (1996), pp. 162–166.

[37] Stephen J. Huston et al. "Neural Encoding of Odors during Active Sampling and in Turbulent Plumes". In: *Neuron* 88 (2015), pp. 1–16.

[38] Karen J. Rossiter. "Structure-odor relationships". In: *Chemical Reviews* 96.8 (1996), pp. 3201–3240.

[39] Kobi Snitz et al. "Predicting Odor Perceptual Similarity from Odor Structure". In: *PLoS Computational Biology* 9.9 (2013).

[40] Manuel Zarzo and David T. Stanton. "Identification of latent variables in a semantic odor profile database using principal component analysis". In: *Chemical Senses* 31.8 (2006), pp. 713–724.

[41] Alexei A. Koulakov et al. "In search of the structure of human olfactory space". In: *Frontiers in Systems Neuroscience* 5.September (2011), pp. 1–8.

[42] Gasper Tkacik et al. "Local statistics in natural scenes predict the saliency of synthetic textures". In: *Proceedings of the National Academy of Sciences of the United States of America* 107.42 (2010), pp. 18149–18154.

[43] Elissa A. Hallem and John R. Carlson. "Coding of odors by a receptor repertoire". In: *Cell* 125.1 (2006), pp. 143–160.

[44] Harumi Saito et al. "Odor Coding by a Mammalian Receptor Repertoire". In: *Science Signaling* 2.60 (Mar. 2009), ra9. arXiv: `arXiv:1011.1669v3`.

[45] Claude E. Shannon. "A mathematical theory of communication". In: *ACM SIGMOBILE Mobile Computing and Communications* 27.July (1948).

[46] Stephen Boyd and Lieven Vandenberghe. *Convex Optimization*. Cambridge University Press, 2004. ISBN: 9780521833783.

[47] Anne L. Calof et al. "Neurogenesis and cell death in olfactory epithelium". In: *Journal of Neurobiology* 30.1 (1996), pp. 67–81. arXiv: `arXiv:1011.1669v3`.

[48] Kensaku Mori, Hiroshi Nagao, and Yoshihiro Yoshihara. "The olfactory bulb: Coding and processing of odor molecule information". In: *Science* 286.5440 (1999), pp. 711–715.

[49] Olivier Rivoire and Stanislas Leibler. "The Value of Information for Populations in Varying Environments". In: *Journal of Statistical Physics* 142 (2011), pp. 1124–1166. arXiv: `arXiv:1010.5092v1`.

[50] Patrick Garrigan et al. "Design of a trichromatic cone array". In: *PLoS Computational Biology* 6.2 (2010), e1000677. arXiv: `77649208745`.

[51] Charles P. Ratliff et al. "Retina is structured to process an excess of darkness in natural scenes". In: *PNAS* 107.40 (2010), pp. 17368–17373.

[52] Stephanie E. Palmer et al. "Predictive information in a sensory population". In: *PNAS* 112.22 (2015), pp. 6908–6913.

[53] Jared M. Salisbury and Stephanie E. Palmer. "Optimal Prediction in the Retina and Natural Motion Statistics". In: *Journal of Statistical Physics* 162.5 (2016), pp. 1309–1323.

[54] Daniel Lewandowski, Dorota Kurowicka, and Harry Joe. "Generating random correlation matrices based on vines and extended onion method". In: *Journal of Multivariate Analysis* 100.9 (2009), pp. 1989–2001.

A Supporting Information

A.1 Choice of sensing matrices

We used three types of sensing matrices in this study. Two were based on experimental data, one using fly receptors [43], and one using mouse and human receptors [44]; and another sensing matrix was based on randomly-generated receptor affinity profiles. These can all be either directly downloaded from our repository on GitHub, `https://github.com/ttesileanu/OlfactoryReceptorDistribution`, or generated using the code available there.

Fly sensing matrix Some of our simulations used a sensing matrix based on *Drosophila* receptor affinities, as measured by Hallem and Carlson [43]. This includes the responses of 24 of the 60 receptor types in the fly against a panel of 110 odorants, measured using single-unit electrophysiology in a mutant antennal neuron. We directly used the values from Table S1 in [43], normalized to obtain the desired SNR (high for Figure 2a, low for Figure 2b, and intermediate values for Figures 2c, and 4b in the main text).

The fly data has the advantage of being more complete than the equivalent datasets in mammals, but since olfactory sensory neurons don't regenerate in the fly, it is less useful for understanding the effects of changing environments.

Mammalian sensing matrix When comparing the results from our simulation to the experimental findings from Ibarra-Soria *et al.* [13], we used a sensing matrix based on mouse and human receptor affinity data from [44]. This was measured using heterologous expression of olfactory genes, and in total it tested 219 mouse and 245 human receptor types against 93 different odorants. However, only 52 mouse receptors and 10 human receptors exhibited detectable responses against any of the odorants, while only 63 odorants activated any receptors. From the remaining $62 \times 63 = 3906$ receptor–odorant pairs, only 335 (about 9%) showed a response, and were assayed at 11 different concentration points. In this paper, we used the values obtained for the highest concentration (3 mM).

The sparsity of the sensing matrix obtained from the Saito *et al.* [44] data makes convergence slow in our simulations. For this reason, we replaced the vanishing entries from this matrix with normally-distributed random variables, with a standard deviation of about 12% of the median value of the non-zero entries.

Random sensing matrices We generated random sensing matrices by first treating the columns of the sensing matrix (*i.e.,* the odorants) like equally-spaced points along a circle, with positions parametrized by a normalized angle $x = \theta/2\pi$. We then generated receptive fields with a Gaussian profile,

$$\phi(x) = \exp\left[-\frac{1}{2}\left(\frac{2\sin\pi(x-x_0)}{\sigma}\right)^2\right], \tag{11}$$

where the expression in the exponent is the planar distance between a point with coordinate x and the center point of the Gaussian, with coordinate x_0. The centers x_0 for the Gaussian profiles for each of the receptors were chosen uniformly at random, and the standard deviation σ was a fixed parameter. As a final step, we shuffled the columns of the resulting sensing matrix to remove the circular ordering of the odorants.

The parameter σ is the tuning width which appears on the x-axis in the main text in Figures 2d and 2e, where it ranges from 0.01 to 0.2. In the main text Figures 4c and 4d, the tuning parameters are 0.05 and 0.8 for top and bottom results, respectively.

A.2 Deriving the expression for the mutual information

Given that we assume a Gaussian distribution for odorant concentrations and that we approximate receptor responses as linear with additive Gaussian noise, eq. 2 in the main text, it follows that the marginal distribution of receptor responses in natural olfactory scenes is also Gaussian. Taking averages of the responses, $\langle r_a \rangle$, and of products of responses, $\langle r_a r_b \rangle$, over both the noise distribution and the odorant distribution, and using eq. 2 from the main text, we get a normal distribution of responses:

$$\mathbf{r} \sim \mathcal{N}(\mathbf{r}_0, R)\,, \tag{12}$$

where the mean response vector $\mathbf{r}_0$ and the response covariance matrix R are given by

$$\begin{aligned} \mathbf{r}_0 &= \mathbb{K} S \mathbf{c}_0 \,, \\ R &= \big[\mathbb{I} + \mathbb{K} Q\big]\, \mathbb{K} \,. \end{aligned} \tag{13}$$

Here, as in eq. 1 in the main text, $\mathbf{c}_0$ is the mean concentration vector, Γ is the covariance matrix of concentrations, and we use the overlap matrix from eq. 5 in the main text, $Q = S\Gamma S^T$. Note that in the absence of noise, the response matrix is simply the overlap matrix Q modulated by the number of OSNs of each type, $R_{\text{noiseless}} = \mathbb{K} Q \mathbb{K}$.

The joint probability distribution over responses and concentrations, $P(\mathbf{r}, \mathbf{c})$, is itself Gaussian. To calculate the corresponding covariance matrix, we need the covariances between responses, $\langle r_a r_b \rangle - \langle r_a \rangle \langle r_b \rangle$, which are just the elements of the response matrix R from eq. (13) above; and between concentrations, $\langle c_i c_j \rangle - \langle c_i \rangle \langle c_j \rangle$, which are the elements of the environment covariance matrix Γ, eq. 1 in the main text. In addition, we need the covariances between responses and concentrations, $\langle r_a c_i \rangle - \langle r_a \rangle \langle c_i \rangle$, which can be calculated using eq. 2 from the main text. We get:

$$(\mathbf{r}, \mathbf{c}) \sim \mathcal{N}\big((\mathbf{r}_0, \mathbf{c}_0), \Lambda\big) \,, \tag{14}$$

with

$$\Lambda = \begin{pmatrix} R & \mathbb{K} S \Gamma \\ \Gamma S^T \mathbb{K} & \Gamma \end{pmatrix} . \tag{15}$$

The mutual information between responses and odors is then given by (see the next section for a derivation):

$$I(\mathbf{r}, \mathbf{c}) = \frac{1}{2} \log \frac{\det \Gamma \det R}{\det \Lambda} \,. \tag{16}$$

From eq. (13) we have

$$\det R = \det(\mathbb{I} + \mathbb{K} Q) \det \mathbb{K} \,, \tag{17}$$

and from eq. (15),

$$\begin{aligned} \det \Lambda &= \det \begin{pmatrix} R & \mathbb{K} S \Gamma \\ \Gamma S^T \mathbb{K} & \Gamma \end{pmatrix} = \det \Gamma \cdot \det(R - \mathbb{K} S \Gamma\, \Gamma^{-1}\, \Gamma S^T \mathbb{K}) \\ &= \det \Gamma \cdot \det(\mathbb{K} + \mathbb{K} Q \mathbb{K} - \mathbb{K} S \Gamma S^T \mathbb{K}) \\ &= \det \Gamma \cdot \det \mathbb{K} \,, \end{aligned} \tag{18}$$

where we used eq. (13) again, and employed Schur's determinant identity (which we also derive in the next section). Thus,

$$I(\mathbf{r}, \mathbf{c}) = \frac{1}{2} \log \frac{\det \Gamma \cdot \det(\mathbb{I} + \mathbb{K} Q) \cdot \det \mathbb{K}}{\det \Gamma \cdot \det \mathbb{K}} = \frac{1}{2} \log \det(\mathbb{I} + \mathbb{K} Q) \,, \tag{19}$$

recovering the result quoted in the main text, eq. 4.

A.3 Details regarding the derivation of the mutual information

Schur's determinant identity The identity for the determinant of a 2×2 block matrix that we used in eq. (18) above can be derived in the following way. First, note that

$$\begin{pmatrix} A & B \\ C & D \end{pmatrix} = \begin{pmatrix} \mathbb{I} & B \\ 0 & D \end{pmatrix} \begin{pmatrix} A - BD^{-1}C & 0 \\ D^{-1}C & \mathbb{I} \end{pmatrix} . \tag{20}$$

Now, from the definition of the determinant it can be seen that

$$\det \begin{pmatrix} A & B \\ 0 & \mathbb{I} \end{pmatrix} = \det \begin{pmatrix} A & 0 \\ C & \mathbb{I} \end{pmatrix} = \det A \,, \tag{21}$$

since all the products involving elements from the off-diagonal blocks must necessarily also involve elements from the 0 matrix. Thus, taking the determinant of eq. (20), we get the desired identity

$$\det \begin{pmatrix} A & B \\ C & D \end{pmatrix} = \det D \cdot \det(A - BD^{-1}C) \,. \tag{22}$$

Mutual information for Gaussian distributions The expression from eq. (16) for the mutual information $I(\mathbf{r}, \mathbf{c})$ can be derived by starting with the fact that I is equal to the Kullback-Leibler divergence from the joint distribution $P(\mathbf{r}, \mathbf{c})$ to the product distribution $P(\mathbf{r})P(\mathbf{c})$. As a first step, let us calculate the Kullback-Leibler divergence between two multivariate normals in n dimensions:

$$D = D_{\mathrm{KL}}(p\|q) = \int p(\mathbf{x}) \log \frac{p(\mathbf{x})}{q(\mathbf{x})}\, d\mathbf{x}\,, \tag{23}$$

where

$$\begin{aligned} p(\mathbf{x}) &= \frac{1}{\sqrt{(2\pi)^n \det A}} \exp\left[-\frac{1}{2}(\mathbf{x}-\mu_A)^T A^{-1}(\mathbf{x}-\mu_A)\right]\,, \\ q(\mathbf{x}) &= \frac{1}{\sqrt{(2\pi)^n \det B}} \exp\left[-\frac{1}{2}(\mathbf{x}-\mu_B)^T B^{-1}(\mathbf{x}-\mu_B)\right]\,. \end{aligned} \tag{24}$$

Plugging the distribution functions into the logarithm, we have

$$\begin{aligned} D = \frac{1}{2}\log\frac{\det B}{\det A} + \frac{1}{2}\int p(\mathbf{x})\Big[&(\mathbf{x}-\mu_B)^T B^{-1}(\mathbf{x}-\mu_B) - \\ &(\mathbf{x}-\mu_A)^T A^{-1}(\mathbf{x}-\mu_A)\Big]\, d\mathbf{x}\,, \end{aligned} \tag{25}$$

where the normalization property of $p(\mathbf{x})$ was used. Using also the definition of the mean and of the covariance matrix, we have

$$\int p(\mathbf{x}) x_i\, d\mathbf{x} = \mu_{A,i}\,, \tag{26a}$$

$$\int p(\mathbf{x}) x_i x_j\, d\mathbf{x} = A_{ij}\,, \tag{26b}$$

which implies

$$\int p(\mathbf{x})\,(\mathbf{x}-\mu)^T C^{-1}(\mathbf{x}-\mu)\, d\mathbf{x} = \mathrm{Tr}(AC^{-1}) + (\mu_A-\mu)^T C^{-1}(\mu_A-\mu) \tag{27}$$

for any vector μ and matrix C. Plugging this into eq. (25), we get

$$\begin{aligned} D = \frac{1}{2}\log\frac{\det B}{\det A} + \frac{1}{2}\left[\mathrm{Tr}(AB^{-1}) - n\right] + \\ \frac{1}{2}(\mu_A-\mu_B)^T B^{-1}(\mu_A-\mu_B)\,. \end{aligned} \tag{28}$$

We can now return to calculating the KL divergence from $P(\mathbf{r}, \mathbf{c})$ to $P(\mathbf{r})P(\mathbf{c})$. Note that, since $P(\mathbf{r})$ and $P(\mathbf{c})$ are just the marginals of the joint distribution, the means of the variables are the same in the joint and in the product, so that the last term in the KL divergence vanishes. The covariance matrix for the product distribution is

$$\Lambda_{\mathrm{prod}} = \begin{pmatrix} R & 0 \\ 0 & \Gamma \end{pmatrix}\,, \tag{29}$$

so the product inside the trace becomes

$$\Lambda\Lambda_{\mathrm{prod}}^{-1} = \begin{pmatrix} R & \dots \\ \dots & \Gamma \end{pmatrix} \begin{pmatrix} R^{-1} & 0 \\ 0 & \Gamma^{-1} \end{pmatrix} = \begin{pmatrix} \mathbb{I} & \dots \\ \dots & \mathbb{I} \end{pmatrix}\,, \tag{30}$$

where the entries replaced by "…" don't need to be calculated because they drop out when the trace is taken. The sum of the dimensions of R and Γ is equal to the dimension, n, of Λ, so that the term involving the trace from eq. (28) also drops out, leaving us with the final result:

$$I = D_{\mathrm{KL}}\left(p(\mathbf{r}, \mathbf{c})\|p(\mathbf{r})p(\mathbf{c})\right) = \frac{1}{2}\log\frac{\det R \det \Gamma}{\det \Lambda}\,, \tag{31}$$

which is the same as eq. (16), which we used in the previous section.

A.4 Deriving the KKT conditions for the information optimum

In order to find the optimal distribution of olfactory receptors, we need to maximize the mutual information from eq. 4 in the main text, subject to constraints. Let us first calculate the gradient of the mutual information with respect to the receptor numbers:

$$\frac{\partial I}{\partial K_a} = \frac{1}{2}\frac{\partial}{\partial K_a}\log\det(\mathbb{I}+\mathbb{K}Q) = \frac{1}{2}\frac{\partial}{\partial K_a}\operatorname{Tr}\log(\mathbb{I}+\mathbb{K}Q)\,. \tag{32}$$

The cyclic property of the trace allows us to use the usual rules to differentiate under the trace operator, so we get

$$\begin{aligned}\frac{\partial I}{\partial K_a} &= \frac{1}{2}\operatorname{Tr}\left[\frac{\partial \mathbb{K}}{\partial K_a}\left(Q^{-1}+\mathbb{K}\right)^{-1}\right] = \frac{1}{2}\sum_{b,c}\frac{\partial\left(K_b\delta_{bc}\right)}{\partial K_a}\left(Q^{-1}+\mathbb{K}\right)^{-1}_{ca} \\ &= \frac{1}{2}\left(Q^{-1}+\mathbb{K}\right)^{-1}_{aa}\,.\end{aligned} \tag{33}$$

We now have to address the constraints. We have two kinds of constraints: an equality constraint that sets the total number of neurons, $\sum K_a = K_{\text{tot}}$; and inequality constraints that ensure that all receptor abundances are non-negative, $K_a \geq 0$. This can be done using the Karush-Tucker-Kuhn (KKT) conditions, which require the introduction of Lagrange multipliers, λ for the equality constraint, and μ_a for the inequality constraints. At the optimum, we must have:

$$\begin{aligned}\frac{\partial I}{\partial K_a} &= \frac{1}{2}\lambda\frac{\partial}{\partial K_a}\left(\sum_b K_b - K_{\text{tot}}\right) - \sum_b \mu_b\frac{\partial}{\partial K_a}K_b \\ &= \lambda - \mu_a\,,\end{aligned} \tag{34}$$

where the Lagrange multipliers for the inequality constraints, μ_a, must be non-negative, and must vanish unless the inequality is saturated:

$$\begin{aligned}\mu_a &\geq 0\,, \\ \mu_a K_a &= 0\,.\end{aligned} \tag{35}$$

Put differently, if $K_a > 0$, then $\mu_a = 0$ and $\partial I/\partial K_a = \lambda/2$; while if $K_a = 0$, then $\partial I/\partial K_a = \lambda/2 - \mu_a \leq \lambda/2$. Combined with eq. (33), this yields

$$\begin{cases}(Q^{-1}+\mathbb{K})^{-1}_{aa} = \lambda\,, & \text{if } K_a > 0, \text{ or} \\ (Q^{-1}+\mathbb{K})^{-1}_{aa} < \lambda\,, & \text{if } K_a = 0.\end{cases} \tag{36}$$

The magnitude of λ is set by imposing the normalization condition in eq. 7b in the main text.

A.5 Deriving the high total neuron number approximation

Suppose we are in the regime in which the total number of neurons is large, and in particular, each of the abundances K_a is large. Then we can perform an expansion of the expression appearing in the KKT equations from eq. (36):

$$(A+\mathbb{K})^{-1} = \mathbb{K}^{-1}(\mathbb{I}+A\mathbb{K}^{-1})^{-1} \approx \mathbb{K}^{-1}(\mathbb{I}-A\mathbb{K}^{-1})\,, \tag{37}$$

where we used the notation $A = Q^{-1}$. This implies

$$\lambda \approx \frac{1}{K_a} - \frac{A_{aa}}{K_a^2}\,. \tag{38}$$

This quadratic equation has only one large solution, and it is given approximately by

$$K_a \approx \frac{1}{\lambda} - A_{aa}\,. \tag{39}$$

Combined with the normalization constraint, $\sum_a K_a = K_{\text{tot}}$, this recovers eq. 8 from the main text.

In the main text we also showed that eq. 8 can give a useful approximation of receptor abundances even for intermediate SNR regimes. In that case, some of the right-hand-sides in eq. (39) might become negative. We can improve the approximation by clipping all values at 0,

$$K_a \approx \max\Big(0, \frac{1}{\lambda} - A_{aa}\Big) . \tag{40}$$

The value for the Lagrange multiplier λ might then need to be adjusted to keep the total number of neurons $\sum_a K_a$ fixed at K_{tot}.

A.6 First receptor type to be activated

When there is only one active receptor, $K_x = K_{\text{tot}}$, $K_{a\neq x} = 0$, the KKT conditions from eq. (36) are automatically satisfied. The receptor that is activated first can be found in this case by calculating the information $I(\mathbf{r}, \mathbf{c})$ using eq. 4 from the main text while assuming an arbitrary index x for the active receptor, and then finding $x = x^*$ that yields the maximum value. Without loss of generality, we can permute the receptor indices such that $x = 1$. We have, when $K_1 = K_{\text{tot}}$,

$$\begin{aligned} I_1(\mathbf{r}, \mathbf{c}) &= \frac{1}{2} \operatorname{Tr} \log(\mathbb{I} + \mathbb{K}Q) = \frac{1}{2} \log\det(\mathbb{I} + \mathbb{K}Q) \\ &= \frac{1}{2} \log \begin{vmatrix} 1 + K_{\text{tot}}Q_{11} & K_{\text{tot}}Q_{12} & \cdots & K_{\text{tot}}Q_{1M} \\ 0 & 1 & & 0 \\ \vdots & & \ddots & \\ 0 & 0 & \cdots & 1 \end{vmatrix} \\ &= \frac{1}{2} \log\big(1 + K_{\text{tot}}Q_{11}\big) . \end{aligned} \tag{41}$$

Thus, in general, the information when only receptor type x is activated is given by

$$I_x(\mathbf{r}, \mathbf{c}) = \frac{1}{2} \log\big(1 + K_{\text{tot}}Q_{xx}\big) , \tag{42}$$

which implies that information is maximized when x matches the receptor corresponding to the highest diagonal value of the overlap matrix Q,

$$x^* = \arg\max Q_{xx} . \tag{43}$$

Another way to think of this result is by employing the usual expression for the capacity of a single Gaussian channel, and then finding the channel that maximizes this capacity.

A.7 Random environment matrices

Generating plausible olfactory environments is difficult because so little is known about natural odor scenes. However, it is reasonable to expect that there will be some strong correlations. This could, for instance, be due to the fact that an animal's odor is composed of several different odorants in fixed proportions, and thus concentrations of these odorants will be correlated.

To generate covariance matrices that have a non-trivial correlation structure, we used a modified form of an algorithm based on partial correlations [54]. The basic idea is that there is a recurrence relation that allows one to eliminate the conditioning variables one by one, so that a set of unconditioned correlations can be obtained by recursively processing the partial correlations.

The distributions from which the partial correlations are drawn in [54] are beta distributions with parameters that depend on the order of the correlations. These are chosen such that the resulting matrices provide a uniform sampling in the space of correlation matrices. However, this leads to samples that are close to diagonal and thus not particularly suitable for modeling olfactory environments. By simply keeping the beta distribution parameters equal to a given fixed value, $\alpha = \beta = \text{const}$, instead of changing depending on the order of the partial correlations, we can instead obtain matrices with a

tunable amount of correlation. More specifically, large values of β lead to almost uncorrelated environments, while small values lead to environments with strong correlations between odorant concentrations. We found this modified algorithm in an entry on the question-and-answer website `Stack Exchange`, at `https://stats.stackexchange.com/q/125020`. This method generates a correlation matrix, in which all the variances are equal to 1. Random variances are then drawn from a lognormal distribution and the rows and columns are multiplied by their square roots, generating a final covariance matrix. The detailed code is available on GitHub, at `https://github.com/ttesileanu/OlfactoryReceptorDistribution`.

When comparing the qualitative results from our model against experiments in which the odor environment changes [13], we used small perturbations of the initial and final environments to estimate error bars on receptor abundances. To generate a perturbed covariance matrix, $\tilde{\Gamma}$, from a starting matrix Γ, we first took the matrix square root: a symmetric matrix M, which obeys

$$\Gamma = MM^T \equiv M^2 \,. \tag{44}$$

We then perturbed M by adding normally-distributed *i.i.d.* values to its elements,

$$\tilde{M}_{ij} = M_{ij} + \sigma\eta_{ij} \,, \tag{45}$$

and recreated a covariance matrix by multiplying the perturbed square root with its transpose,

$$\tilde{\Gamma} = \tilde{M}\tilde{M}^T \,. \tag{46}$$

This approach ensures that the perturbed matrix $\tilde{\Gamma}$ remains a valid covariance matrix—symmetric and positive-definite—which wouldn't be guaranteed if the random perturbation was added directly to Γ. We chose the magnitude σ of the perturbation so that the error bars in our simulations are of comparable magnitude to those in the experiments.

A.8 Deriving the dynamical model

To turn the maximization requirement into a dynamical model, we turn to a gradient ascent argument. Given the current abundances K_a, we demand that they change in proportion to the corresponding components of the information gradient, plus a Lagrange multiplier to impose the constraint on the total number of neurons:

$$\dot{K}_a = 2\alpha\left(\frac{\partial I}{\partial K_a} - \lambda\right) = \alpha\big[\big(Q^{-1} + \mathbb{K}\big)^{-1}_{aa} - \lambda\big] \,. \tag{47}$$

The brain does not have direct access to the overlap matrix Q, but it could measure the response covariance matrix R from eq. (13). Thus, we can write the dynamics as

$$\begin{aligned}\dot{K}_a &= \alpha\Big\{\big[Q(\mathbb{I} + \mathbb{K}Q)^{-1}\big]_{aa} - \lambda\Big\} \\ &= \alpha\Big\{\big[\mathbb{K}^{-1}(R\mathbb{K}^{-1} - \mathbb{I})\mathbb{K}R^{-1}\big]_{aa} - \lambda\Big\} \\ &= \alpha\Big\{K_a^{-1} - \lambda - R_{aa}^{-1}\Big\} \,.\end{aligned} \tag{48}$$

These equations do not yet obey the non-negativity constraint on the receptor abundances. The divergence in the K_a^{-1} term would superficially appear to ensure that positive abundances stay positive, but there is a hidden quadratic divergence in the response covariance term, R_{aa}^{-1}; see eq. (13). To ensure that all constraints are satisfied while avoiding divergences, we multiply the right-hand-side of eq. (48) by K_a^2, yielding

$$\dot{K}_a = \alpha\big[K_a - K_a^2\big(\lambda + R_{aa}^{-1}\big)\big] \,, \tag{49}$$

which is the same as eq. 9 from the main text.

If we keep the Lagrange multiplier λ constant, the asymptotic value for the total number of neurons K_{tot} will depend on the statistical structure of olfactory scenes. If instead we want to enforce the constraint from eq. 7b in the main text for a predetermined K_{tot}, we can promote λ itself to a dynamical variable,

$$\frac{d\lambda}{dt} = \beta\left[\sum_a K_a - K_{\text{tot}}\right] , \tag{50}$$

where β is another learning rate. Provided that the dynamics of λ is sufficiently slow compared to that of the neuronal populations K_a, this will tune the experience-independent component of the neuronal death rate until the total population stabilizes at K_{tot}.

A.9 Multiple glomeruli with the same affinity profile

In mammals, the axons from neurons expressing a given receptor type can project to anywhere from 2 to 16 different glomeruli. Here we show that in our setup, information transfer only depends on the total number of neurons of a given type, and not on the number of glomeruli to which they project.

The key observation is that mutual information, eq. 3 in the main text, is unchanged when the responses and/or concentrations are modified by monotonic transformations. In particular, linear transformations of the responses do not affect the information values. Suppose that we have a case in which two receptors p and q have identical affinities, so that $S_{pi} = S_{qi}$ for all odorants i. We can then form linear combinations of the corresponding glomerular responses,

$$\begin{aligned} r_+ &= r_p + r_q = (K_p + K_q) \sum_i S_{pi} c_i + \eta_p \sqrt{K}_p + \eta_q \sqrt{K}_q \,, \\ r_- &= K_q r_p - K_p r_q = \eta_p K_q \sqrt{K}_p - \eta_q K_p \sqrt{K}_q \,, \end{aligned} \tag{51}$$

and consider a transformation that replaces (r_p, r_q) with (r_+, r_-). Since r_- is pure noise, *i.e.,* it does not depend on the concentration vector $\mathbf{c}$ in any way, it has no effect on the mutual information.

We have thus shown that the amount of information that M receptor types contain about the environment when two of the receptors have identical affinity profiles is the same as if there were only $M-1$ receptor types. The two redundant receptors can be replaced by a single one with an abundance equal to the sum of the abundances of the two original receptors. (Remember that in eq. 2 in the main text we had assumed that the responses are normalized such that the variance of η is unity. This is automatically satisfied for the r_+ response from eq. (51) because the sum of two Gaussian variables with the same mean is Gaussian itself and has a variance equal to the sum of the variances of the two variables. This means that the noise term in eq. (51) is equivalent to $\eta_+ \sqrt{K_p + K_q}$, with $\eta_+ \sim \mathcal{N}(0,1)$.)

A.10 Interpretation of diagonal elements of inverse overlap matrix

In the main text we saw that the diagonal elements of the inverse overlap matrix Q^{-1}_{aa} were well-correlated with the abundances of OSNs K_a. Recall that the overlap matrix was defined as $Q = S\Gamma S^T$, where S is the sensing matrix, and Γ is the environment covariance matrix (see eq. 1 and eq. 2). In the main text, we suggested that a possible explanation for this correlation is based on the relation between inverse covariance matrices (also called precision matrices) and partial correlations.

More specifically, as noted around eq. (13) above, the overlap matrix Q and the response covariance matrix are related: in particular, Q is equal to R when there is a single receptor of each type ($K_a = 1$) and there is no noise ($\eta = 0$ in eq. 2). Thus, the inverse overlap matrix $A = Q^{-1}$ is effectively a precision matrix. Diagonal elements of a precision matrix are inversely related to the corresponding diagonal elements of the corresponding covariance matrix, but they are also monotonically-related to goodness-of-fit parameters that show how well each variable can be linearly predicted from all the others. Since receptor responses that either do not fluctuate much or whose values can be guessed based on the responses from other receptors are not very informative, we would expect that abundances K_a are low when the corresponding diagonal elements of the inverse overlap matrix A_{aa} are high, which is what we see. In the following we give a short derivation of the connection between the diagonal elements of precision matrices and goodness-of-fit parameters.

Let us thus work in the particular case in which there is one copy of each receptor and there is no noise, so that $Q = R$, *i.e.,* $Q_{ij} = \langle r_i r_j \rangle - \langle r_i \rangle \langle r_j \rangle$. Without loss of generality, we focus on calculating the first diagonal element of the inverse overlap matrix, A_{11}, where $A = Q^{-1}$. For notational convenience, we will also denote the mean-centered first response variable by $y \equiv r_1 - \langle r_1 \rangle$, and the subsequent ones by $x_a \equiv r_{a+1} - \langle r_{a+1} \rangle$. Then the covariance matrix Q can be written in block form

$$Q = \begin{pmatrix} \langle y^2 \rangle & \langle y \mathbf{x}^T \rangle \\ \langle y \mathbf{x} \rangle & M \end{pmatrix} , \tag{52}$$

where M is

$$M = \langle \mathbf{x}\mathbf{x}^T \rangle \,. \tag{53}$$

Using the definition of the inverse together with Laplace's formula for determinants, we get

$$A_{11} = \frac{\det M}{\det Q} \,. \tag{54}$$

Using the Schur determinant identity (derived above) on the block form (eq. (52)) of the matrix Q,

$$\begin{aligned} A_{11} &= \frac{\det M}{\det M \cdot \det\big[\langle y^2 \rangle - \langle y\mathbf{x}^T \rangle M^{-1} \langle y\mathbf{x} \rangle\big]} \\ &= \frac{1}{\langle y^2 \rangle - \langle y\mathbf{x}^T \rangle M^{-1} \langle y\mathbf{x} \rangle} \,, \end{aligned} \tag{55}$$

where we used the fact that the argument of the second determinant is a scalar.

Now, consider approximating the first response variable y by a linear function of all the others:

$$y = \mathbf{a}^T \mathbf{x} + q \,, \tag{56}$$

where q is the residual. Note that we do not need an intercept term because we mean-centered our variables, $\langle y \rangle = \langle x \rangle = 0$. Finding the coefficients $\mathbf{a}$ that lead to a best fit (in the least-squares sense) requires minimizing the variance of the residual, and a short calculation yields

$$\mathbf{a}^* = \arg\min_{\mathbf{a}} \langle q \rangle^2 = \arg\min_{\mathbf{a}} (y - \mathbf{a}^T \mathbf{x})^2 = M^{-1} \langle y\mathbf{x} \rangle \,, \tag{57}$$

where M is the same as the matrix defined in eq. (53).

The coefficient of determination ρ^2 is defined as the ratio of explained variance to total variance of the variable y,

$$\begin{aligned} \rho^2 &= \frac{\langle (\mathbf{a}^{*T} \mathbf{x})^2 \rangle}{\langle y^2 \rangle} = \frac{\mathbf{a}^{*T} \langle \mathbf{x}\mathbf{x}^T \rangle \mathbf{a}^*}{\langle y^2 \rangle} = \frac{\langle y\mathbf{x}^T \rangle M^{-1} M M^{-1} \langle y\mathbf{x} \rangle}{\langle y^2 \rangle} \\ &= \frac{\langle y\mathbf{x}^T \rangle M^{-1} \langle y\mathbf{x} \rangle}{\langle y^2 \rangle} \,. \end{aligned} \tag{58}$$

Comparing this to eq. (55), we see that

$$A_{11} = \frac{1}{\langle y^2 \rangle} \frac{1}{1 - \rho^2} \,, \tag{59}$$

showing that indeed the diagonal elements of the precision matrix are monotonically-related to the goodness-of-fit parameter ρ^2 that indicates how well the corresponding variable can be linearly predicted by all the other variables. In addition, the inverse dependence on the variance of the response $\langle y \rangle^2$ shows that variables that do not fluctuate much (low $\langle y \rangle^2$ and thus high A_{11}) tend to have low abundances.